REFERENCES

1. D.K. Jacob, S.C. Dunn, and M.G. Moharam, Interference approach applied to dual-grating dielectric resonant grating reflection filters, Opt Lett 26 (2001), 1749.
2. M.S. Saremi and R. Magnusson, Particle swarm optimization and its application to the design of diffraction grating filter, Opt Lett 32 (2007), 894.
3. A. Coves, B. Gimeno, J. Gil, M.V. Andres, A.A.S. Blas, and V.E. Boria, Full-wave analysis of dielectric frequency-selective surfaces using a vectorial modal method, IEEE Trans Antennas Propag 52 (2004), 2091–2099.
4. Y. Kanamori, K. Hane, H. Sai, and H. Yugami, 100nm Period silicon antireflection structures fabricated using a porous alumina membrane mask, Appl Phys Lett 78 (2001), 142–143.
5. T. Glaser, S. Schroter, H. Bartelt, H.J. Fuchs, and E.B. Kley, Diffractive optical isolator made of high-efficiency dielectric gratings only, Appl Opt 41 (2002), 3558–3566.
6. H. Kikuta, Y. Ohira, and K. Iwata, Achromatic quarter-wave plates using the dispersion of form birefringence, Appl Opt 36 (1997), 1566–1572.
7. H. Li, G.T. Liu, P.M. Varangis, T.C. Newell, A. Stintz, B. Fuchs, K.J. Malloy, and L.F. Lester, 150-nm Tuning range in a grating-coupled external cavity quantum-dot laser, IEEE Photonics Technol Lett 12 (2000), 759–761.
8. J. Kim, P.K. Kondratko, S.L. Chuang, G. Walter, and N. Holonyak, Jr., Experimental demonstration of the polarization-dependent photon-mediated carrier redistribution in tunneling injection InP quantum-dot lasers with external-grating feedback, Appl Phys Lett 90 (2007), 211102.
9. L. Pajewski, R. Borghi, G. Schettini, F. Frezza, and M. Santarsiero, Design of a binary grating with subwavelength features that acts as a polarizing beam splitter, Appl Opt 40 (2001), 5898–5905.
10. M.G. Moharam, E.B. Grann, D.A. Pommet, and T.K. Gaylord, Formulation for stable and efficient implementation of the rigorous coupled-wave analysis of binary gratings, J Opt Soc Am A 12 (1995), 1068–1076.
11. P. Lalanne and G.M. Morris, Highly improved convergence of the coupled-wave method for TM polarization, J Opt Soc Am A 13 (1996), 779–784.
12. M.G. Moharam and T.K. Gaylord, Diffraction analysis of dielectric surface-relief gratings, J Opt Soc Am 72 (1982), 1385–1392.
13. J.R. Andrewartha, G.H. Derrick, and R.C. McPhedran, A modal theory solution to diffraction from a grating with semi-circular grooves, Opt Acta 28 (1981), 1177–1193.
14. I.C. Botten, M.S. Craig, R.C. McPhedran, J.L. Adams, and J.R. Andrewartha, The dielectric lamellar diffraction grating, Opt Acta 28 (1981), 413–428.
15. P. Sheng, R.S. Stepleman, and P.N. Sanda, Exact eigenfunctions for square-wave gratings: Application to diffraction and surface-plasmon calculations, Phys Rev B 26 (1982), 2907–2916.
16. T. Clausnitzer, T. Kampfe, E.-B. Kley, A. Tunnermann, U. Peschel, A.V. Tishchenko, and O. Parriaux, An intelligible explanation of highly-efficient diffraction in deep dielectric rectangular transmission gratings, Opt Express 13 (2005), 10448.
17. K. Yokomori, Dielectric surface-relief gratings with high diffraction efficiency, Appl Opt 23 (1984), 2303–2310.
18. H.J. Gerritsen and M.L. Jepsen, Rectangular surface-relief transmission gratings with a very large first-order diffraction efficiency (95%) for unpolarized light, Appl Opt 37 (1998), 5823–5829.
19. B. Wang, C. Zhou, S. Wang, and J. Feng, Polarizing beam splitter of a deep-etched fused-silica grating, Opt Lett 32 (2007), 1299.
20. CST Microwave Studio 2009 [Online], Available at: http://www.cst.com.

BROADBAND ELECTRICALLY SMALL ANTENNA USING TWO ELECTROMAGNETICALLY COUPLED RADIATORS

Chihyun Cho,[1] Ikmo Park,[2] and Hosung Choo[3]

[1] Institute of Advanced Technologies, Samsung Thales, Yongin, Korea

[2] Department of Electrical and Computer Engineering, Ajou University, Suwon, Korea

[3] School of Electronic and Electrical Engineering, Hongik University, Seoul, Korea; Corresponding author: hschoo@hongik.ac.kr

Received 1 August 2009

ABSTRACT: *We propose an electrically small antenna that achieves broad bandwidth with small antenna size. This antenna is composed of a hemispherical disk-loaded monopole and a hemispherically wound helix to maximize the disk loading effect and the electromagnetic coupling between the two radiating elements in a given space. The fabricated antenna is 10.7 cm in size (*$\mathrm{kr} = 0.449$*) and exhibits a measured −3 dB bandwidth of about 30% for a center frequency of 200 MHz. The antenna also achieves a radiation efficiency of over 85% and a transmission loss similar to that of a conventional λ/4 monopole, despite the fact that size of the antenna is about 30% that of the λ/4 monopole.* © 2010 Wiley Periodicals, Inc. Microwave Opt Technol Lett 52: 1369–1372, 2010; Published online in Wiley InterScience (www.interscience.wiley.com). DOI 10.1002/mop.25164

Key words: *small; antenna; broadband*

1. INTRODUCTION

To increase the portability of wireless systems, a compact handheld transceiver and small broadband antenna is highly desirable. However, as the size of an antenna is reduced, its input resistance drops drastically and its reactance changes capacitive, and as a result, that makes it difficult to match with other RF systems. Also, the reduced antenna size increases the quality factor as the stored energy around the antenna is more increased compared with that of the radiating energy. The increased quality factor decreases the antenna's bandwidth and radiating efficiency, resulting in poor antenna performances.

Recently, for preventing degradation of bandwidth and efficiency, the small EM-coupled monopole antenna was introduced [1, 2]. The reported antenna has two small radiators and they are electromagnetically coupled to each other and thus produces two resonances closely spaced in frequency. As a result, antenna achieves about 20% of bandwidth ($|\Gamma| < -10$ dB) while its electrical size is reduced to $\mathrm{kr} = 0.56$.

In this article, to further improve the broadband characteristics of the EM-coupled antenna, we propose a novel antenna structure that consists of a hemispherical disk and a helix to more efficiently use the given space. The size of the proposed antenna is $\mathrm{kr} = 0.449$ and the measured bandwidth ($|\Gamma| < -3$ dB) is about 30% where the center frequency is 200 MHz. The radiation efficiency is over 85%, and the measured transmission loss is similar to that of λ/4 monopole in the operating frequency band.

2. ANTENNA DESIGN

The proposed antenna is composed of a disk-loaded monopole and a helix, closely spaced to achieve a broad bandwidth characteristic through the electromagnetic coupling between the two radiating elements. The disk structure of the disk-loaded monopole takes a hemispherical shape to reduce the quality factor,

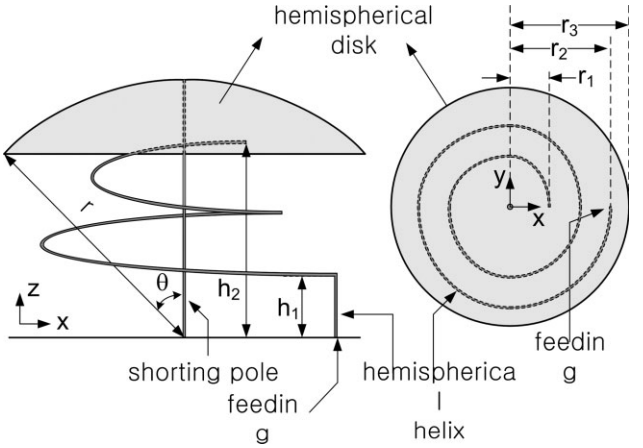

Figure 1 Configuration of the proposed antenna

Figure 2 Photo of the built antenna

and as a result, increases the bandwidth by effectively using the given space. The hemispherical structure can also improve the radiation efficiency by distributing the induced current over a larger area of the disk surface than a circular or a square disk [1–4]. Another radiating element of the helix is wound around the shorting pole of the disk-loaded monopole to maximize the magnetic coupling between the shorted pole and the helix. In addition, the hemispherical structure of the helix magnifies the capacitive coupling between the helix and the concave inner surface of the disk.

Figure 1 shows the geometry and the design parameters of the proposed antenna. The loaded disk is placed over an imaginary hemisphere of radius r with its size r_3 determined by the angle θ. A shorting pole with radius of 1 mm connects the center of the disk to the ground. The helix is wound around the shorting pole with N turns between the height of h_1 and h_2, where the radius of the helix is gradually reduced from r_2 to r_1. The starting point of the helix at h_1 is directly connected to the feed point, which is fed by a single-ended coaxial line. The coordinate of each point on the hemispherical helix can be obtained using the following equations:

$$x = r_2 \cos\left(\frac{\alpha}{2\pi N}\phi\right)\cos\phi.$$

$$y = r_2 \cos\left(\frac{\alpha}{2\pi N}\phi\right)\sin\phi.$$

$$z = \left(\frac{h_2 - h_1}{\sin\alpha}\right)\sin\left(\frac{\alpha}{2\pi N}\phi\right) + h_1.$$

where, $\alpha = \cos^{-1}\left(\frac{r_1}{r_2}\right)$.

Design parameters for the proposed antenna were determined using a genetic algorithm in conjunction with the FEKO software package by EM Software and Systems [5, 6]. The optimized design parameters are as follows: $r = 10.71$ cm, $\theta = 43.4°$, $h_1 = 2.56$ cm, $h_2 = 5.52$ cm, $r_1 = 4.37$ cm, $r_2 = 6.34$ cm, $r_3 = 7.36$ cm, and $N = 1$. The optimized antenna has an electrical size of $kr = 0.449$ at the frequency of 200 MHz. To validate the optimized antenna design, the antenna was constructed as shown in Figure 2. The hemispherical disk is made of aluminum, and the helix and the shorting pole of the disk are made of brass wire of 1 mm radius. The antenna is built on a ground plane of size 1.8×1.8 m^2, and a plastic cylinder with low dielectric constant is used to support each radiating element.

3. RESULTS

Figure 3 shows the measured and simulated return loss of the proposed antenna. The simulation is performed using the FEKO software and exhibits a bandwidth of 28% [($|\Gamma| < -3$ dB) (VSWR < 5.8) from 176 to 232 MHz], and the measurement taken with an Agilent E5071A network analyzer was 30.5% [($|\Gamma| < -3$ dB) from 168 to 229 MHz]. This measurement agrees fairly well with the simulation result. The bandwidth of the proposed antenna is compared with other small antennas in Table 1. The size of the proposed antenna is reduced about 20% compared with that of the EM-coupled monopole antenna in Refs. 1, 2 by applying the hemispherical structures while the bandwidth performance is similarly maintained.

By examining current distributions using the numerical simulation, we confirmed that the first dip in the return loss at about 180 MHz is caused by the hemispherically loaded disk, and the second dip at about 220 MHz comes from the hemispherically wound helix. Although only the helix is fed by a coaxial line, both of the radiating elements resonate because they are electromagnetically very tightly coupled. The two resonances closely spaced in frequency provide the wideband characteristic of the antenna.

Usually, an extremely small antenna shows poor radiation characteristics, such as a low-radiation efficiency due to its large

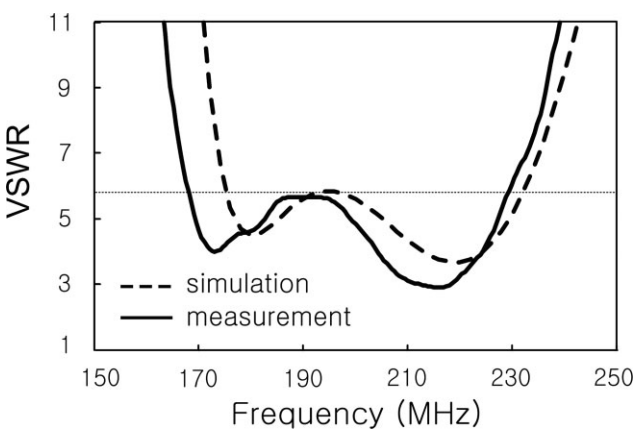

Figure 3 Measured (—) and simulated (- - - -) return loss of the proposed antenna

TABLE 1 Comparisons of Bandwidths for Some Electrically Small Antennas

	Proposed Antenna	EM-Coupled Monopole [2]	Disk-Loaded Monopole with Parallel Strip [4]	Conical-Folded Monopole [7]	Multielement Disk-Loaded Monopole [3]
kr	0.449	0.563	0.63	0.71	1.0
Bandwidth (%)	30.5	30.2	22	28.6	82

conduction and dielectric losses. To examine these radiation characteristics, we measured the radiation efficiency and the transmission loss of the proposed antenna. The simulated (dash–dot) and measured (square marks) radiation efficiencies found using the Wheeler cap method [8, 9] are represented in Figure 4. Both of the results show a high-radiation efficiency of over 85% even with an electrically small size of kr = 0.449. This high-radiation efficiency is achieved by the increased area of the current path with spherical disk loading. In the same figure, the measured transmission loss of the proposed antenna (solid line) is also compared with that of a conventional $\lambda/4$ monopole (dashed line) with a height of 35.5 cm that resonates at 200 MHz. The dipole of ETS-Lindgren [10] is used as the transmitting antenna and the distance between the AUT and transmitter is set to 15 m (10 λ). The resulting transmission loss of the proposed antenna is similar to that of the conventional monopole (the difference is less than 3 dB in the operating frequency band), although the antenna is only about 30% as large as the conventional monopole.

Finally, we measure the radiation pattern of the proposed antenna after the antenna is mounted on a ground plate of 1×1 m^2. The normalized radiation patterns at 180 and 220 MHz are represented in Figures 5(a) and 5(b), respectively. The measurements match fairly well with the simulation and are quite similar to that of the conventional monopole on a finite ground plane.

4. CONCLUSION

In this article, we proposed a novel electrically small antenna, which consists of a hemispherically shaped disk and a hemispherically wound helix that maximize the electromagnetic coupling between the two radiating elements. Measurements show that at the center frequency of 200 MHz the antenna achieves a bandwidth of about 30%, a radiation efficiency of over 85%, and a transmission loss similar to that of a conventional monopole.

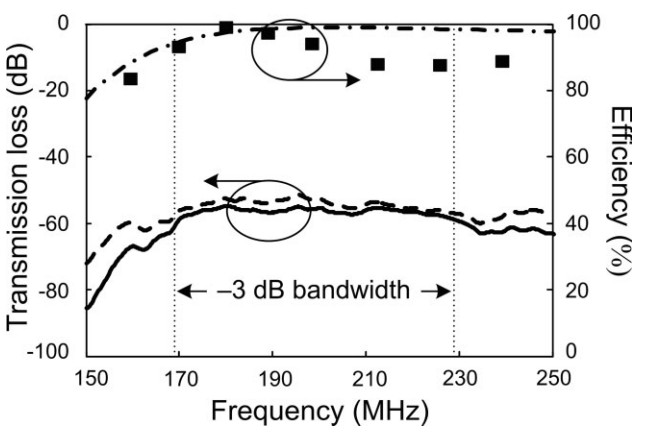

Figure 4 Measured (■) radiation efficiency, simulated (-·-·-·-) radiation efficiency, measured transmission loss (—) of the proposed antenna, and measured transmission loss (- - - -) of the $\lambda/4$ conventional monopole

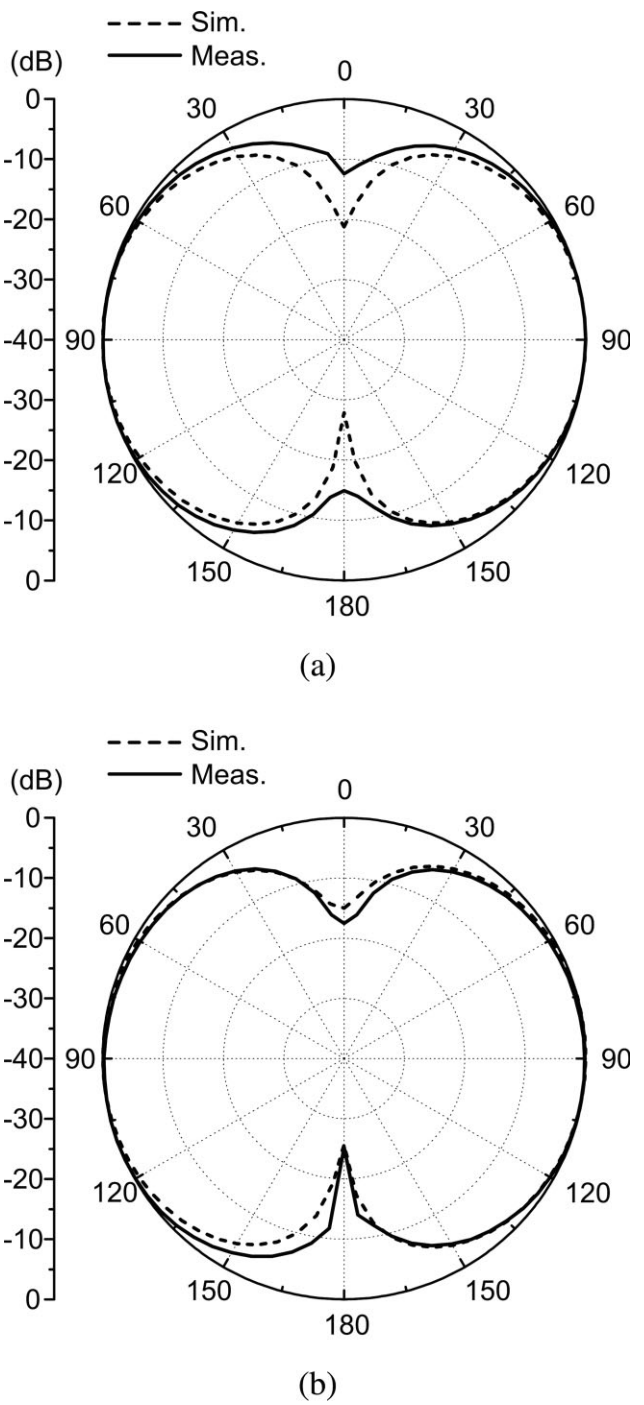

Figure 5 Measured (—) and simulated (- - - -) radiation pattern of the proposed antenna

ACKNOWLEDGMENTS

This work was supported by the IT R&D program of MKE/IITA. [2009-F-042-01, A Study on Mobile Communication System for Next-Generation Vehicles with Internal Antenna Array].

REFERENCES

1. J.H. Jung and I. Park, Electromagnetically coupled small broadband monopole antenna, IEEE Antennas Wireless Propag Lett 2 (2003), 349–351.
2. J.H. Jung, H. Choo, and I. Park, Design and performance of small electromagnetically coupled monopole antenna for broadband operation, IET Microwave Antennas Propag 1 (2007), 536–541.
3. G. Goubau, N. Puri, and F. Schwering, Diakoptic theory for multielement antennas, IEEE Trans Antennas Propag 30 (1982), 15–26.
4. H.D. Foltz, J.S. McLean, and G. Crook, Disk-loaded monopoles with parallel strip elements, IEEE Trans Antennas Propag 46 (1998), 1894–1896.
5. Y. Rahmat-Samii and E. Michelssen, Electromagnetic optimization by genetic algorithm, Wiley, New York, NY, 1999.
6. FEKO Suite 5.3. Available at: www.feko.info.
7. J.A. Dobbins and R.L. Rogers, Folded conical helix antenna, IEEE Trans Antennas Propag 49 (2001), 1777–1781.
8. H.A. Wheeler, The radiansphere around a small antenna, Proc IRE, 47 (1959), 1325–1331.
9. H. Choo, R. Rogers, and H. Ling, On the Wheeler cap measurement of the efficiency of microstrip antenna, IEEE Trans Antennas Propag 53 (2007), 2328–2332.
10. ETS LINDGREN Adjustable dipole Model 3121C. Available at: www.ets-lindgren.com/manuals/3121C.pdf.

MINIATURIZED BAND-PASS FILTER FOR BROADBAND APPLICATIONS

M. F. Karim,[1] A. Q. Liu,[2] L. C. Ong,[1] and Yong-Xin Guo[3]

[1] Institute for Infocomm Research, Agency for Science, Technology and Research (A *Star), 1 Fusionopolis Way, #21-01, Connexis North, Singapore 138632; Corresponding author: kfaeyz@i2r.a-star.edu.sg

[2] School of Electrical and Electronic Engineering, Nanyang Technological University, Nanyang Avenue, Singapore

[3] Department of Electrical and Computer Engineering, National University of Singapore, Singapore

Received 8 August 2009

ABSTRACT: *This article reports a new compact design of band-pass filter for broadband applications. It has a compact design with two bended short stubs of quarter-wavelength and a connecting stub of half-wavelength, which result in the design of a broadband filter. The filter is fabricated on silicon substrate using surface micromachining process. The fractional bandwidth of band-pass filter reported is around 0.9–4 GHz. The rejection at upper and lower pass band edge is greater than 35 dB, and the insertion loss is 2.4 dB. The area of the novel filter is* $(\lambda_g/4)^2$ *at the centre frequency of the bandpass, whereas the area of the filter realized using the nonbending stubs and connecting lines is* $2(\lambda_g/4)^2$ *for the same band pass characteristics.* © 2010 Wiley Periodicals, Inc. Microwave Opt Technol Lett 52: 1372–1375, 2010; Published online in Wiley InterScience (www.interscience.wiley.com). DOI 10.1002/mop.25177

Key words: *broadband filter; RF MEMS; CPW; band-pass filter; airbridges*

1. INTRODUCTION

Bandpass filters with small size and light weight are the fundamental components of communication systems. Recently, coplanar waveguide (CPW) structure has gained substantial research interests because of the advantages such as lower dispersion, ease in connection of series, and shunt connections, no via holes and easier to integrate with solid stated devices [1]. Several CPW band-pass filters with different topologies have been proposed and investigated. The CPW band-pass filter based on capacitively [2] or inductively [3] coupled half wavelength resonators may achieve only loose coupling; thus, they are more suitable for narrow band applications. The broadside end-coupled band-pass filter proposed by [4] achieves larger coupling and wider band width, but the uniplanar structure of CPW would be destroyed. An LC-coupled CPW band-pass filter with quarter wave length resonators was examined [5], but low frequencies, these filters occupy considerable amount of area due to the use of several quarter wave length resonators. The reduced size CPW band-pass filter based on folder stubs [1] features sharp roll off at upper pass band edge, but the roll-off at lower pass band edge is not good. The recent developments in micromachining process have allowed for the possibility of fabricating filters on silicon substrate with compact size [6–9].

In this article, a new reduced size broadband CPW band-pass filter using two bended $\lambda_g/4$ short stubs and a bended $\lambda_g/2$ connecting lines between stubs is proposed. This filter has the merit of compact size, high cut off rate, and low insertion loss in pass-band. The filter has been designed, simulated, and fabricated on silicon substrate using surface micromachining process. The measured and simulated results are compared and good agreement has been observed between them.

2. DESIGN OF THE BANDPASS FILTER

The wide band CPW band-pass filter is shown in Figure 1. The structure is composed of two bended short stubs and bended connecting line that is in the form of square loop. The bended short stubs have a length of $l_2 = \lambda_g/4$ at the centre frequency of the band pass. Unlike the conventional $\lambda_g/4$ filter, the connecting lines between the stubs has a length of $l_1 = \lambda_g/2$ to obtain wider band pass. The bending of the stubs makes the design more compact with respect to the conventional (nonbended) structure. The short ended stubs have the same characteristics as the connecting line. Their characteristic impedance are $Z_1 = 65\ \Omega$. The impedance is high to compensate for the air bridges at the corner of the CPW bends. Airbridges are placed to suppress the unwanted coupled-slotline mode, which tends to radiate and results in resonance peaks in the passband; thus, it will result in obtaining an adequate filter performance.

The filter bandwidth is dependent on the center connecting line, denoted by l_1. An expression can be calculated in terms of l_1 to find the bandwidth dependent relationship. Using the ABCD parameters, the desired length is given by

$$\begin{bmatrix} A & B \\ C & D \end{bmatrix} = \begin{bmatrix} 1 & 0 \\ j & 1 \end{bmatrix} \begin{bmatrix} \cos\beta l_1 & jZ_1 \sin\beta l_1 \\ jY \sin\beta l_1 & \cos\beta l_1 \end{bmatrix} \begin{bmatrix} 1 & 0 \\ j & 1 \end{bmatrix} \quad (1)$$

$$\begin{bmatrix} A & B \\ C & D \end{bmatrix} = \begin{bmatrix} \cos\beta l_1 - Z_1 \sin\beta l_l & jZ_1 \sin\beta l_1 \\ 2jY \cos\beta l_1 & \cos\beta l_1 - Z_1 \sin\beta l_1 \end{bmatrix} \quad (2)$$

Using the ABCD to S-parameters transformation, the required $S21$ can be calculated as

$$S_{21} = \frac{2}{2\cos\beta l_1 - 2Z_1 \sin\beta l_1 + j(\sin\beta l_1 + 2Z_1 \cos\beta l_1)} \quad (3)$$

Figure 2 shows how the length, l_1, can be varied according to the required bandwidth. When the length is $\lambda_g/4$, the